Design and Analysis of Three-Dimensional Printing of A Porous Titanium Scaffold

Chunxi Yang (chunxi_yang@163.com)
Renji Hospital
Jiajie Yang
Nantong Haimen People's Hospital
Xiaojian Shi
Nantong Haimen People's Hospital
Meihua Shen
Nantong Haimen People's Hospital
Kaibing Shi
Nantong Haimen People's Hospital
Lingjie Shen
Nantong Haimen People's Hospital

Research Article

Keywords: Bone defect, Metal scaffold, Three-dimensional printing, Titanium, Safety factor, Compressive strength

Posted Date: May 21st, 2021

DOI: https://doi.org/10.21203/rs.3.rs-525195/v1

Version of Record: A version of this preprint was published at BMC Musculoskeletal Disorders on August 2nd, 2021. See the published version at https://doi.org/10.1186/s12891-021-04520-1.

DESIGN AND ANALYSIS OF THREE-DIMENSIONAL PRINTING OF A POROUS TITANIUM SCAFFOLD

Jiajie Yang[1] , Xiaojian Shi[1], Meihua Shen[1], Kaibing Shi[1], Lingjie Shen[1], and Chunxi Yang[2]

【 Abstract 】 **Objective** To develop suitable structural designs for the three-dimensional (3-D) printing of a porous titanium scaffold to fill bone defects in knee joints. Pore diameter and mechanic strength are key factors for the 3-D printing of porous titanium scaffolds. **Methods** Fifteen different pore unit structural models of titanium scaffolds were designed with 3-D printing computer software; five different scaffold shapes were designed: imitation diamond-60° , imitation diamond-90° , imitation diamond-120° , regular tetrahedron and regular hexahedron. Each structural shape was evaluated with three pore diameters 400μm, 600μm and 800μm, and fifteen types of cylindrical models(diameter: 20mm; height: 20mm). Autodesk Inventor software was used determine the strength and safety of the models by simulating simple strength acting on the knee joints. We analyzed the data and found suitable models for 3-D printing of porous titanium scaffolds. **Results** Fifteen different types of pore unit structural models were evaluated under positive pressure; the compressive strength was lower when the pore diameter(400μm, 600μm and 800μm) was larger, except for the regular tetrahedron structure. Under lateral pressure, the compressive strength was also lower when the pore diameter(400μm, 600μm and 800μm) was larger. Under torsional pressure, the strength of the imitation diamond structure was similar when the pore diameter(400μm, 600μm and 800μm) was larger, and the strengths of the regular tetrahedron and regular hexahedron structures were lower when the pore diameter(400μm, 600μm and 800μm) was larger. In each case, the compressive strength of the regular hexahedron structure was highest, that of the regular tetrahedron was second highest, and that of the imitation diamond structure was relatively low. Fifteen types of cylindrical models under a set force were evaluated, and the sequence of comprehensive compressive strength, from strong to weak was: regular hexahedron> regular tetrahedron> imitation diamond-120° > imitation diamond-90° > imitation diamond-60° . The compressive strength of cylinder models was higher when the pore diameter was smaller. **Conclusion** The compressive strength differed among titanium scaffolds with different pore structures. The pore diameter and shapes of the pore structure were important factors influencing the compressive strength. The models of regular hexahedron, regular tetrahedron and imitation diamond-120° appeared to meet the conditions of large pore diameters and high compressive strength. The strength of each structure was lower when the pore diameter(400μm, 600μm and 800μm) was larger.

【Key words】Bone defect; Metal scaffold; Three-dimensional printing; Titanium;

1. Nantong Haimen People's Hospital, 1201 Beijing Road, Haimen District, Nantong City, Jiangsu Province, China, 226100
2. Renji Hospital Affiliated to Shanghai Jiaotong University School of Medicine, 145 Shandong Zhong Lu, Shanghai, China, 200001
Corresponding author: Chunxi Yang, E-mail：chunxi_yang@163.com

Safety factor; Compressive strength

1 Introduction

The complexity of revision total hip arthroplasty (THA) and revision total knee arthroplasty (TKA) is increasing, and important effects include bone defects due to infection, osteolysis, original implant loosening or tumor excision. Clinically, bone loss has been addressed with methods such as cement, autogenous bone grafts, and artificial implants[1, 2]. However, autogenous bone grafts are painful and limited, by complications[3]. Bone cement can lead to complications of absorption poisoning, bone absorption poisoning, bone absorption and allergies[4]. In recent years, artificial implant materials, such as calcium phosphate[5], ceramic[6] and metal[7], have been developed. Porous titanium scaffolds generated with three-dimensional (3-D) printing have great advantages for the control of porosity, pore diameter, pore volume, spatial arrangement and other surface features. Titanium has also been used in bone implants. Some studies have shown that 3-D printing of porous titanium is conducive to bone differentiation and new bone formation[8, 9]. 3-D printing of porous titanium metaphyseal cones has previously been applied to revision TKA[10].

3-D printing technology, which is based on computer-aided design data, uses powder chromatography as a layer-by-layer printing method to quickly create objects with a complex 3-D structure[11]. Compared with the traditional production technology, such as porous scaffolds, 3-D printing technology has greater advantages in the control of the scaffold porosity, pore diameter, pore volume, spatial arrangement and other surface properties[12]. 3-D printing technology has been used in many industries, including the medical industry, such as for orthopedic surgery and bone defects, to make models and help doctors better understand complex anatomy and pathology[13-17].

At present, many scaffold materials are available for bone tissue engineering, including metal, ceramic and polymer materials[18]. Among them, metal is used in bone tissue engineering because of its high strength, high load capacity, shape memory, inertness and superelasticity. Common metal scaffolds include tantalum, titanium and titanium-nickel alloy.

Tantalum is a biocompatible material with good tissue compatibility with human tissue, causing almost no side effects. Therefore, this metal is widely used in medical clinics[19, 20]. The tantalum scaffold is currently prepared by chemical vapor deposition and infiltration into the carbon skeleton[21]. Tantalum powder can also be obtained by selective laser melting to generate the structure, which is a positive dodecahedron, with a porosity of 80% of the 3-D structure of a porous tantalum scaffold[22]. However, the tantalum scaffold is expensive, and its strong oxidation and high melting point lead to costly and difficult processing. The production cost is high, the methods are limited, and the tantalum powder shape is irregular; therefore, it difficult to use 3-D printing to generate tantalum scaffolds.

Titanium has very high corrosion resistance, low density, and the highest strength / weight ratio of metals in addition to being non-magnetic. Titanium and titanium alloy materials also have good biomechanical properties and biocompatibility. Therefore,

titanium is widely used in orthopedic implants[23]. Compared with tantalum, titanium powder (Ti6Al4V powder is commonly used) is the ideal 3-D printing material for spherical particles, with an average diameter of 45μm[24]. The elastic modulus of pure titanium is approximately 108 GPa, and the elastic modulus of titanium alloys is approximately 6 times that of cortical bone. With prolonged implantation, titanium can cause a stress shielding effect (over time, bone will atrophy or even fracture due to the decreased mechanical tension), leading to biomechanical failure. The porous titanium scaffold produced by 3-D printing technology has a lower modulus of elasticity compared to dense titanium[25], and the 3-D pore structure of the 3-D printed scaffold is conducive to the growth of bone tissue[26]. Furthermore, the cytotoxicity of titanium and titanium alloys is very low[27]. Titanium scaffolds have been used in clinical medicine and bone surgery, and porous titanium acetabular cups have been used in THA[28]. Titanium and alloys can be made with 3-D printing technology to produce the appropriate porosity, aperture and spatial arrangement of porous titanium scaffolds, and 3-D printing can be combined with CT scans to establish models[29], or produce a variety of geometric shapes of the porous scaffold to repair complex bone defects. Therefore, 3-D printing of a porous titanium scaffold has good prospects for bone tissue engineering, making it a good research subject.

Porous metal scaffolds implanted in the human knee will be subjected to a variety of forces, such as positive, lateral and torsional pressure. Porous metal scaffolds have a certain multi-directional compressive strength, but they must also have appropriate pore size and porosity. In this study, fifteen titanium scaffold models with different pore structures and fifteen cylindrical models were designed. Finite element analysis was carried out by simulating stress on the knee joint. The results were converted into force or a safety factor. The design models with large pore sizes and high compressive strength were screened out, which could provide references for the further production of porous titanium scaffolds with the 3-D printing technique.

2 Materials and Methods

2.1 Scaffold Model Design

Five types of unit structures were designed using Autodesk Inventor software (Inventor 2016, Autodesk Inc. San Rafael, California, USA), imitation diamond-60°, imitation diamond-90°, imitation diamond-120°, regular tetrahedron and regular hexahedron. The diameter of the bracket bar was 400 μm. Each type of unit structure has three pore sizes 400μm, 600μm and 800μm, and the aperture is set as shown in **Fig. 1**. The fifteen kinds of unit structures were aligned to obtain a cylinder with a diameter of 20 mm and a height of 20 mm (cylinder diameter and height were finely adjusted for overall integrity).

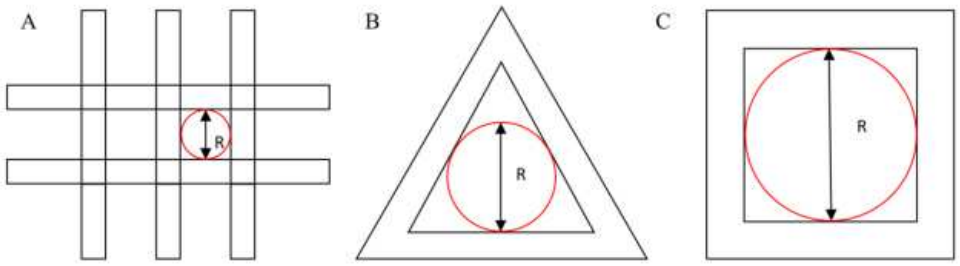

Fig. 1 (a) Overall top view of the imitation diamond unit structure; R is the size of the aperture. (b) Regular tetrahedron unit structure has a diameter R in either side. (c) Size of the aperture R is the inscribed circle diameter on either side of the regular hexahedral unit structure.

2.2 Finite Element Analysis

The positive pressure, lateral pressure and torsional pressure were applied to fifteen kinds of unit structures and the corresponding fifteen kinds of cylindrical models with ABAQUS software (ABAQUS 2016, Simulia Inc. Providence, Rhole Island, USA). Finite element analysis was carried out to obtain the mechanical properties and compare the data.

The configuration of the computer used to run the Autodesk Inventor software and the ABAQUS software included a CPU model: Intel Core i7 6700HQ, quad-core eight threads, 256GB solid state + 1TB hard disk, 16G memory, NVIDIA GeForce GTX 1060 graphics card, and Win10 system.

2.2.1 Setting and Analysis of Unit Structure Model

When the positive pressure, lateral pressure and torsional pressure were applied to the fifteen kinds of unit structures, and when the minimum safety factor of the model was greater than or equal to 1, the force was the maximum pressure the unit structure could bear (accurate to 0.5N). When the unit structure was under positive pressure, lateral pressure and torsional pressure, a fixed surface was selected and a force was applied to the offside of the fixed side. The unit structure and force are shown in **Fig. 2**. The maximum forces of each unit structure in the safe state obtained by software analysis were compared.

2.2.2 Safety Factor

The safety factor is the ratio of the ultimate stress to the allowable stress. The safety factor is the strength margin, considering factors that accurately calculate the load and stress, the importance of the work of the machine, and the reliability of the material. The value is greater than or equal to 1 (less than 1 indicates permanent deformation)[30, 31]. When the computer simulated the applied force, the point with the minimum value of the safety factor of models (**Fig.3**) was determined, which was the point where the model was most likely to be damaged.

2.2.3 Setting and Analysis of Cylindrical Model

Five types of cylindrical models are shown in **Fig. 4**. The pressure applied to the fifteen kinds of cylindrical models was set such that the pressure on the knee was approximately twice the weight of the adult (approximately 60kg). When an adult is standing on one leg, the knee is subjected to a stress of approximately 3 ~ 4 times the person's weight. The pressure on the knees when climbing stairs is about 3 to 6 times of body weight[32]. When the person kicks the ball, the twisting force is approximately 3000N- 4000N. Therefore, when the positive, lateral and torsional pressures were applied to the fifteen kinds of cylindrical models, they were applied with 1 times, 3 times and 5 times the positive pressure and 1 times and 3times the lateral pressure, and the torsional pressure applied was 2000N, 3000N and 4000N. Then, the safety factors were obtained using the ABAQUS software analysis under different values for various forces and compared.

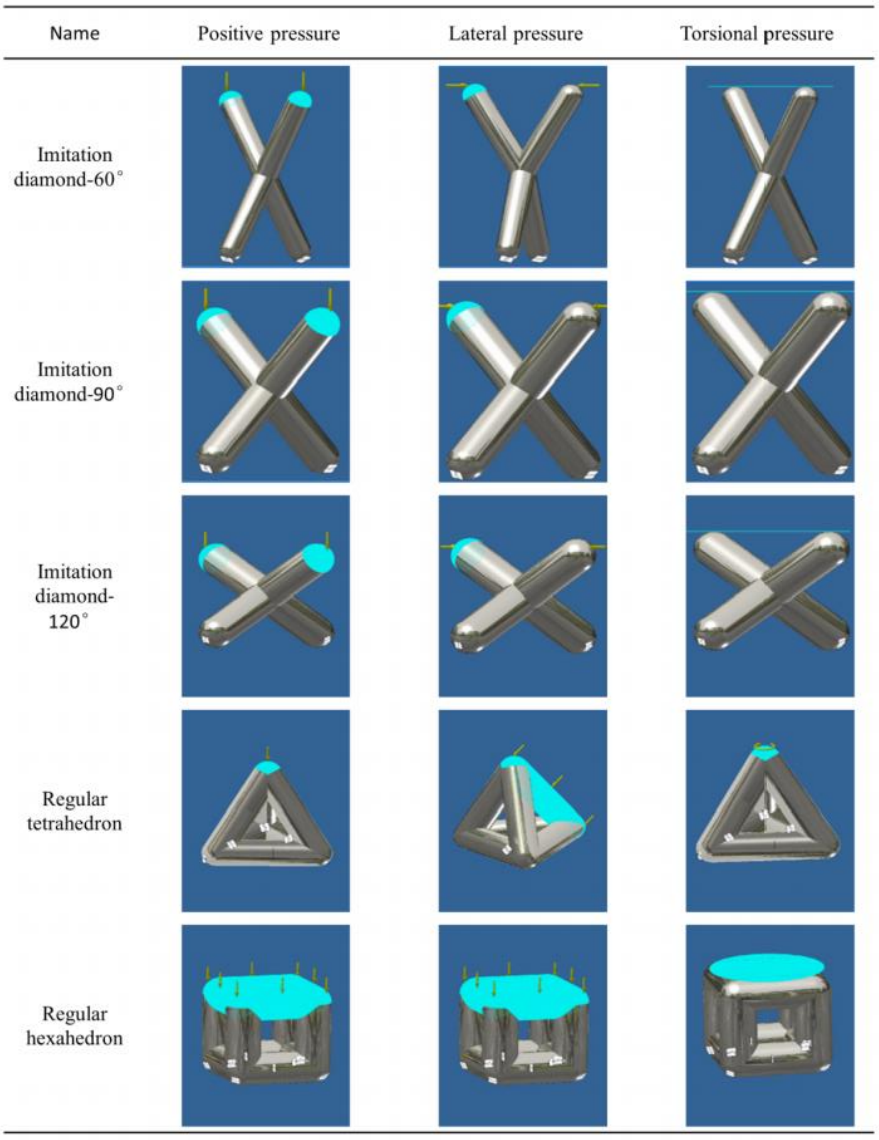

Fig. 2 Schematic of different unit structures and applied pressure.

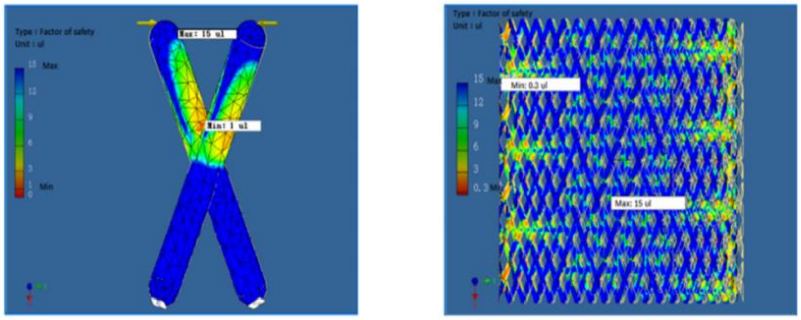

Fig. 3 Unit structure and cylindrical structure of imitation diamond-60° under lateral pressure (600N); blue indicates security, and red indicates danger. The reddest point occurred when the safety factor was the smallest.

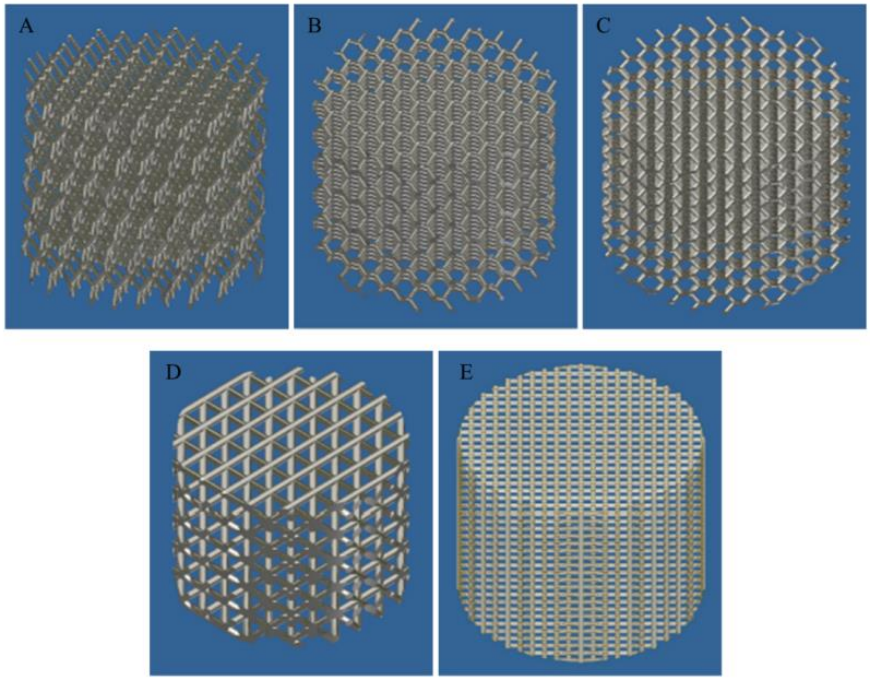

Fig.4 The five types of Cylindrical model. (A) Imitation diamond-60°; (B) imitation diamond-90°; (C) imitation diamond-120; (D) regular tetrahedron; (E) hexahedron.

3 Results and Analysis

3.1 Results and Analysis of Unit Structure Model

The maximum positive pressure values that could be sustained on the fifteen kinds of unit structures in the safety state are shown in **Table 1**. The maximum lateral pressure values are shown in **Table 2**, and the maximum torsional pressure values are shown in **Table 3**. Through the analysis of the data in the table, the following conclusions can be drawn:

① Under positive pressure, the maximum force of the imitation diamond and the

regular hexahedron structure decreased with increasing pore diameter, the maximum force of the regular tetrahedron structure didn't decrease with increasing pore diameter, and the maximum forces of the regular tetrahedron and the regular hexahedron structures were much larger than that of the imitation diamond structure, and the compressive strength of the regular hexahedron structure was the highest.

Table 1 When the safety factor is greater than or equal to 1, the unit structure can withstand the maximum positive pressure (accurate to 0.5N)

Positive pressure (Unit：N）	400μm	600μm	800μm
Imitation diamond-60°	10.5	8.0	6.0
Imitation diamond-90°	8.0	8.5	7.0
Imitation diamond-120°	11.0	9.0	7.5
Regular tetrahedron	88.5	92.0	93.0
Regular hexahedron	185.0	165.0	155.0

Table 2 When the safety factor is greater than or equal to 1, the unit structure can withstand the maximum lateral pressure (accurate to 0.5N)

Lateral pressure (Unit：N）	400μm	600μm	800μm
Imitation diamond-60°	3.0	2.0	1.5
Imitation diamond-90°	5.0	4.0	4.0
Imitation diamond-120°	8.5	7.5	6.0
Regular tetrahedron	65.0	45.0	39.5
Regular hexahedron	185.0	165.0	155.0

Table 3 When the safety factor is greater than or equal to 1, the unit structure can withstand the maximum torsional pressure (accurate to 0.5N)

Torsional pressure (Unit：N）	400μm	600μm	800μm
Imitation diamond-60°	9.0	8.5	8.5
Imitation diamond-90°	7.0	9.5	10.0
Imitation diamond-120°	11.5	11.5	11.5
Regular tetrahedron	4.5	4.5	4.0
Regular hexahedron	51.5	53.5	46.5

② Under the lateral pressure, the maximum force of the five kinds of unit structures decreased with increasing pore diameter, and the maximum forces of the regular tetrahedron and regular hexahedron structures wre much larger than that of the imitation diamond structure. The compressive strength of the regular hexahedron structure was the highest.
③ Under the torsional pressure, the maximum force of the imitation diamond-90° structure increased with increasing pore diameter. The maximum force of the other structure did not change with the pore diameter. The regular hexahedron structure had the greatest torsional resistance. And the regular tetrahedron structure had the smallest torsional resistance.
④ In the comprehensive analysis of positive pressures, the order of compressive capacity of the five types of unit models, from strong to weak, was regular hexahedron > regular tetrahedron > imitation diamond-120° > imitation diamond-90° > imitation diamond-60°.
⑤ In the lateral pressure comprehensive analysis, the order of the compressive capacity of the five types of unit models from strong to weak, was regular hexahedron > regular tetrahedron > imitation diamond-120° > imitation diamond-90° > imitation diamond-60°.
⑥ In the comprehensive analysis of the torsional pressure, the order of the compressive capacity of the five types of unit models, from strong to weak, was regular hexahedron> imitation diamond-120°> imitation diamond-90°> imitation diamond-60°> regular tetrahedron.

3.2 Results and Analyses of Cylindrical Model

The safety factors for the fifteen cylindrical models given the positive, lateral and torsional pressures are shown in **Tables 4-8**. Through the analysis of the data in the tables, the following conclusions could be drawn:
① Under the positive, lateral and torsional pressures, the safety factors of the imitation diamond, the regular tetrahedron and the regular hexahedron models decreased with increasing pore diameter.
② Under positive pressure, considering factors such as the force, pore diameter and safety factor, the order of the compressive capacity of the five types of cylindrical models, from strong to weak, was regular hexahedron > regular tetrahedron > imitation diamond-90° > imitation diamond-60° > imitation diamond-120°.
③ Under the lateral pressure or torsional pressure, considering factors such as the force, pore diameter and safety factor, the order of the compressive capacity of the five types of cylindrical models, from strong to weak, was regular hexahedron > regular tetrahedron > imitation diamond-120° > imitation diamond-90° > imitation diamond-60°.
④ Based on the above points, the order of the comprehensive compressive capacity of the five types of cylindrical models, from strong to weak, was regular hexahedron > regular tetrahedron > imitation diamond-120° > imitation diamond-90°> imitation diamond-60°. The smaller the pore diameter in each type of cylindrical model, the

greater the compressive strength.

Table 4 Minimum safety factor for the imitation diamond-60° cylindrical model under different pressures

Minimum safety factor	Pore diameter (μm)	400	600	800
Positive pressure	600N	2.63	0.96	0.81
	1800N	0.88	0.33	0.05
	3000N	0.53	0.18	0.16
Lateral pressure	600N	0.30	0.25	0.15
	1800N	0.10	0.08	0.05
Torsional pressure	2000N	1.43	0.28	0.35
	3000N	0.95	0.18	0.24
	4000N	0.72	0.72	0.18

Table 5 Minimum safety factor for the imitation diamond-90° cylindrical model under different pressures

Minimum safety factor	Pore diameter (μm）	400	600	800
Positive pressure	600N	2.74	1.19	1.58
	1800N	0.91	0.40	0.53
	3000N	0.55	0.24	0.32
Lateral pressure	600N	0.59	0.81	0.40
	1800N	0.20	0.27	0.13
Torsional pressure	2000N	2.86	0.87	1.19
	3000N	1.91	0.58	0.80
	4000N	1.43	0.43	0.60

Table 6 Minimum safety factor for the imitation diamond-120° cylindrical model under different pressures

Minimum safety factor	Pore diameter (μm)	400	600	800
Positive pressure	600N	1.47	1.64	0.69
	1800N	0.49	0.55	0.23

	3000N	0.29	0.33	0.14
Lateral pressure	600N	1.43	1.40	1.14
	1800N	0.48	0.47	0.38
Torsional pressure	2000N	2.00	3.22	1.33
	3000N	1.33	2.14	0.89
	4000N	1.00	1.61	0.67

Table 7 Minimum safety factor for the regular tetrahedron cylindrical model under different pressures

Minimum safety factor	Pore diameter (μm)	400	600	800
Positive pressure	600N	15.00	1.52	0.56
	1800N	4.34	0.51	0.19
	3000N	2.60	0.30	0.11
Lateral pressure	600N	6.17	3.50	1.57
	1800N	2.06	1.17	0.52
Torsional pressure	2000N	1.99	0.94	0.49
	3000N	1.33	0.63	0.32
	4000N	1.00	0.47	0.24

Table 8 Minimum safety factor for the regular hexahedron cylindrical model under different pressures

Minimum safety factor	Pore diameter (μm)	400	600	800
Positive pressure	600N	15.00	8.30	15.00
	1800N	15.00	2.77	10.53
	3000N	11.50	1.66	6.32
Lateral pressure	600N	7.06	0.26	6.55
	1800N	2.35	0.09	2.18
Torsional pressure	2000N	5.69	0.79	8.27
	3000N	3.80	0.36	8.27
	4000N	3.80	0.27	4.14

4 Discussion

In the revision of THA and TKA, bone defects are among the important problems to be solved. Treatments of bone defects include autologous bone grafts, allogeneic bone grafts, bone cement and the implantation of artificial materials. Autologous bone graft leads to pain, bone loss and other complications, and the quantity of available tissue is limited. Allogeneic bone grafts reduce bone conduction and osteoinduction, but they can also transmit infectious diseases. Bone cement can be absorbed,causing poisoning, bone resorption, allergies and other complications. At present, a variety of artificial materials have been used to treat bone defects, including metals because they have favorable characteristics. Titanium and its alloys are very good implant materials, because they have high strength, high toughness, good corrosion resistance and good biocompatibility, facilitating their use in clinical medicine. However, the elastic modulus of compact titanium is relatively high, and long-term implantation will cause a stress shielding effect. 3-D printe titanium scaffolds can effectively reduce the elastic modulus, and 3-D printing is highly controllable, enabling the design and production of porous titanium scaffolds with a variety of shapes, pores and pore diameters. Porous titanium scaffolds used to treat bone defects, especially at the knee joints, require high compressive strength, considering the growth of cells in the body, large pore diameters (the pore diameter of osteoblast attachment, differentiation and growth has a range of 200-500μm or even larger[33]), good biocompatibility and other characteristics[34]. Using the 3-D printing technique, the porous titanium scaffold models with different structures and different pore diameters can be designed and analyzed by software. The data are then compared and analyzed to determine whether the model has sufficiently large pore diameter and compressive strength.

The factors that affect the growth of osteoblasts are pore diameter and, factors such as pore diameter, connectivity, pore shape and porosity[35]. In this study, Autodesk Inventor software was used to design the unit structures and cylindrical models with different structures and different pore diameters. The lower limit of the pore diameter was 400μm, which ensured that the pore diameter of the scaffold was large enough. There were five different types of unit structures, each with different shapes of pores. Any of the structures of the scaffold holes could be connected to any other (**Fig. 3**). Then finite element analyses were used to select the appropriate models and provide a reference for producing entities with 3-D printing for analysis.

The positive pressure for the imitation diamond unit structure could be analyzed with the simple model in **Fig. 5**.

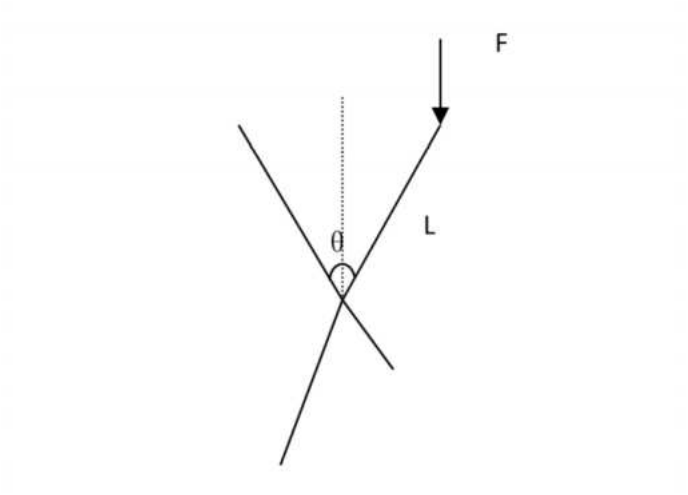

Fig.5 Positive pressure on the imitation diamond unit structure

The length of the bracket bar was L, the angle between the two bars was θ, the pressure on the bar end was F, the moment of the bracket center point was M, and the following formula could be obtained[36]:

$$M=FL\sin\frac{\theta}{2}$$

From the above formula, when the moment M of the bracket center point was constant, the compressive strength at the point where the bracket was most vulnerable was constant; when θ was constant, L was larger and F was smaller. When L was constant, θ was larger ($0° <\theta <180°$) and F was smaller.

Therefore, for the imitation diamond structure, when the pore diameter was consistent, the angle θ was larger and the force F was smaller. When the angle between the two bars was constant, the pore diameter was larger, L was larger, and the force F was smaller.. However, because the pore diameter of the imitation diamond was the same, θ was larger but L was smaller; therefore, it was not sufficient to use this formula for analysis.

For the regular tetrahedron, the vertex moment M was constant, while at the same time, there were three bars bearing pressure; thus compared to the imitation diamond structure, the regular tetrahedron could withstand greater force.

For the regular hexahedron, the force was in the longitudinal direction of the bar, which was the compressive strength of the titanium bar, and it could therefore withstand the greatest force.

There are some shortcomings in this study: ① Compared with dense titanium,3-D printed porous titanium scaffolds have a lower modulus of elasticity, but this study did not analyze the elastic modulus. ② This study did not measure or analyze the porosity, surface area or other factors. ③ The porous titanium scaffold used to fill knee bone defects is not simply under positive, lateral or torsional pressure, but may also be subject to various directions of the various pressures from various directions; this study failed to analyze this complex condition. ④Due to the different pore diameters of unit

structures contained in the fixed-size cylindrical model, the complete unit structure may not be retained at the edge of the model when intercepting, resulting in some data inconsistent with the theory. For example, in Table 8, when the 600μm pore diameter models were subjected to force, the data obtained were not in the middle.⑤This study only used software to design and simulate forces; the obtained data are only a reference for further entity production and testing. Biocompatibility and osteoblast attachment, differentiation and growth on the 3-D printed porous titanium scaffold require further studies.

The porous titanium scaffold made by 3-D printing technology has good biomechanical properties and biocompatibility compared to titanium and its alloys. Compared to the space-holder technology[37], foaming method[38] and other methods, 3-D printing technology can better control of the porosity, pore diameter, pore volume, spatial arrangement and other surface properties of scaffolds. For treating bone defects in the revision of TKA, the 3-D printed porous titanium scaffold can provide a potentially effective clinical solution that is worthy of further exploration.

5 Conclusions

This study evaluated 3-D printed porous titanium scaffolds with fifteen different pore structures under positive, lateral and torsional pressures. The order of the comprehensive compressive capacity of the five types of cylindrical models was regular hexahedron > regular tetrahedron > imitation diamond-120° > imitation diamond-90° >imitation diamond-60°, and for each type of cylinder, the smaller the pore size, the greater the compressive strength. The regular hexahedron, regular tetrahedron and imitation diamond-120° models appear to meet the conditions of large pore diameter and high compressive strength. In addition, the strength of each structure was smaller when the pore diameter(400μm, 600μm and 800μm) was larger.

Declarations

Ethics approval and consent to participate

Not applicable.

Consent for publication

Availability of data and materials

Materials described in the manuscript, including all relevant raw data, can be freely available to any scientist and reader wishing to use them for non-commercial purposes, without breaching participant confidentiality. The datasets used and/or analysed during the current study are available from the corresponding author on reasonable

request. All data generated or analysed during this study are included in this published article.

Competing interests

The authors declare that they have no competing interests.

Funding

This work was supported by the Shanghai Science and Technology Committee Guidance Project (16411971700); Fundamental Research Funds for the Central Universities, Subject Crossing (1501219095); and National Natural Science Foundation of China (81101344/H0604).

Authors' contributions

Chunxi Yang contributed to the conception of the study; Jiajie Yang performed the experiment; Jiajie Yang and Chunxi Yang contributed significantly to analysis and manuscript preparation; Jiajie Yang performed the data analyses and wrote the manuscript; Xiaojian Shi, Meihua Shen, Kaibing Shi and Lingjie Shen helped perform the analysis with constructive discussions.

Acknowledgments

The authors thank School of Biomedical Engineering, Shanghai Jiao Tong University, for finite element analysis.

References

1. Fedorka CJ, Chen AF, Pagnotto MR, Crossett LS, Klatt BA: **Revision total knee arthroplasty with porous-coated metaphyseal sleeves provides radiographic ingrowth and stable fixation**. *Knee surgery, sports traumatology, arthroscopy : official journal of the ESSKA* 2017.
2. Villatte G, Erivan R, Salles G, Pereira B, Galvin M, Descamps S, Boisgard S: **Acetabular bone defects in THA revision: Reconstruction using morsellised virus-inactivated bone allograft and reinforcement ring. Seven-year outcomes in 95patients**. *Orthopaedics & traumatology, surgery & research : OTSR* 2017.
3. Costa Mendes L, Sauvigne T, Guiol J: **Morbidity of autologous bone harvesting in implantology: Literature review from 1990 to 2015**. *Revue de stomatologie, de chirurgie maxillo-faciale et de chirurgie orale* 2016, **117**(6):388-402.
4. Stathopoulos I, Andrianopoulos N, Paschaloglou D, Tsarouchas I: **Revision total knee arthroplasty due to bone cement and metal hypersensitivity**. *Arch Orthop Traum Su* 2017, **137**(2):267-271.
5. Inzana JA, Olvera D, Fuller SM, Kelly JP, Graeve OA, Schwarz EM, Kates SL, Awad HA: **3D printing of composite calcium phosphate and collagen scaffolds for bone regeneration**. *Biomaterials* 2014, **35**(13):4026-4034.
6. Bose S, Vahabzadeh S, Bandyopadhyay A: **Bone tissue engineering using 3D printing**. *Mater Today* 2013, **16**(12):496-504.
7. Li X, Wang L, Yu XM, Feng YF, Wang CT, Yang K, Su D: **Tantalum coating on porous Ti6Al4V scaffold using chemical vapor deposition and preliminary biological evaluation**. *Mat Sci Eng*

C-Mater 2013, **33**(5):2987-2994.

8. Zhou X, Zhang D, Wang M, Zhang D, Xu Y: **Three-Dimensional Printed Titanium Scaffolds Enhance Osteogenic Differentiation and New Bone Formation by Cultured Adipose Tissue-Derived Stem Cells Through the IGF-1R/AKT/Mammalian Target of Rapamycin Complex 1 (mTORC1) Pathway**. *Medical science monitor : international medical journal of experimental and clinical research* 2019, **25**:8043-8054.
9. Zheng Y, Han Q, Wang J, Li D, Song Z, Yu J: **Promotion of Osseointegration between Implant and Bone Interface by Titanium Alloy Porous Scaffolds Prepared by 3D Printing**. *ACS biomaterials science & engineering* 2020, **6**(9):5181-5190.
10. Faizan A, Bhowmik-Stoker M, Kirk AE, Krebs VE, Harwin SF, Meneghini RM: **Development and Verification of Novel Porous Titanium Metaphyseal Cones for Revision Total Knee Arthroplasty**. *The Journal of arthroplasty* 2017.
11. Hong S, Sycks D, Chan HF, Lin S, Lopez GP, Guilak F, Leong KW, Zhao X: **3D Printing of Highly Stretchable and Tough Hydrogels into Complex, Cellularized Structures**. *Advanced materials* 2015, **27**(27):4035-4040.
12. Roseti L, Parisi V, Petretta M, Cavallo C, Desando G, Bartolotti I, Grigolo B: **Scaffolds for Bone Tissue Engineering: State of the art and new perspectives**. *Materials science & engineering C, Materials for biological applications* 2017, **78**:1246-1262.
13. Tetsworth K, Block S, Glatt V: **Putting 3D modelling and 3D printing into practice: virtual surgery and preoperative planning to reconstruct complex post-traumatic skeletal deformities and defects**. *Sicot-J* 2017, **3**:16.
14. Rasperini G, Pilipchuk SP, Flanagan CL, Park CH, Pagni G, Hollister SJ, Giannobile WV: **3D-printed Bioresorbable Scaffold for Periodontal Repair**. *Journal of dental research* 2015, **94**(9 Suppl):153S-157S.
15. Shaunak S, Dhinsa BS, Khan WS: **The Role of 3D Modelling and Printing in Orthopaedic Tissue Engineering: A Review of the Current Literature**. *Current stem cell research & therapy* 2017, **12**(3):225-232.
16. Wong KC: **3D-printed patient-specific applications in orthopedics**. *Orthop Res Rev* 2016, **8**:57-66.
17. Belvedere C, Siegler S, Fortunato A, Caravaggi P, Liverani E, Durante S, Ensini A, Konow T, Leardini A: **New comprehensive procedure for custom-made total ankle replacements: Medical imaging, joint modeling, prosthesis design, and 3D printing**. *Journal of orthopaedic research : official publication of the Orthopaedic Research Society* 2019, **37**(3):760-768.
18. Heller M, Bauer HK, Goetze E, Gielisch M, Ozbolat IT, Moncal KK, Rizk E, Seitz H, Gelinsky M, Schrder HC *et al*: **Materials and scaffolds in medical 3D printing and bioprinting in the context of bone regeneration**. *Int J Comput Dent* 2016, **19**(4):301-321.
19. M DEF, Gobbato EA, Noce D, Cavallari F, Fioretti A: **Clinical and radiographic evaluation of single tantalum dental implants: a prospective pilot clinical study**. *ORAL & implantology* 2016, **9**(Suppl 1/2016 to N 4/2016):38-44.
20. Potter GD, 3rd, Abdel MP, Lewallen DG, Hanssen AD: **Midterm Results of Porous Tantalum Femoral Cones in Revision Total Knee Arthroplasty**. *The Journal of bone and joint surgery American volume* 2016, **98**(15):1286-1291.
21. Paganias CG, Tsakotos GA, Koutsostathis SD, Macheras GA: **Osseous integration in porous tantalum implants**. *Indian journal of orthopaedics* 2012, **46**(5):505-513.

22. Wauthle R, van der Stok J, Amin Yavari S, Van Humbeeck J, Kruth JP, Zadpoor AA, Weinans H, Mulier M, Schrooten J: **Additively manufactured porous tantalum implants**. *Acta biomaterialia* 2015, **14**:217-225.
23. Gao Y, Ou Y, Deng Q, He B, Du X, Li J: **Comparison between titanium mesh and autogenous iliac bone graft to restore vertebral height through posterior approach for the treatment of thoracic and lumbar spinal tuberculosis**. *PloS one* 2017, **12**(4):e0175567.
24. Li JP, de Wijn JR, Van Blitterswijk CA, de Groot K: **Porous Ti6Al4V scaffold directly fabricating by rapid prototyping: Preparation and in vitro experiment**. *Biomaterials* 2006, **27**(8):1223-1235.
25. El-Hajje A, Kolos EC, Wang JK, Maleksaeedi S, He Z, Wiria FE, Choong C, Ruys AJ: **Physical and mechanical characterisation of 3D-printed porous titanium for biomedical applications**. *Journal of materials science Materials in medicine* 2014, **25**(11):2471-2480.
26. Felgueiras HP, Decambron A, Manassero M, Tulasne L, Evans MD, Viateau V, Migonney V: **Bone tissue response induced by bioactive polymer functionalized Ti6Al4V surfaces: In vitro and in vivo study**. *Journal of colloid and interface science* 2017, **491**:44-54.
27. Tuomi JT, Bjorkstrand RV, Pernu ML, Salmi MV, Huotilainen EI, Wolff JE, Vallittu PK, Makitie AA: **In vitro cytotoxicity and surface topography evaluation of additive manufacturing titanium implant materials**. *Journal of materials science Materials in medicine* 2017, **28**(3):53.
28. Perticarini L, Zanon G, Rossi SM, Benazzo FM: **Clinical and radiographic outcomes of a trabecular titanium acetabular component in hip arthroplasty: results at minimum 5 years follow-up**. *BMC musculoskeletal disorders* 2015, **16**:375.
29. Spetzger U, Frasca M, Konig SA: **Surgical planning, manufacturing and implantation of an individualized cervical fusion titanium cage using patient-specific data**. *European spine journal : official publication of the European Spine Society, the European Spinal Deformity Society, and the European Section of the Cervical Spine Research Society* 2016, **25**(7):2239-2246.
30. Sibgatullin KE, Sibgatullin ES: **Safety Factor of Anisotropic Bars in the Space of Generalized Forces**. *Mech Compos Mater* 2017, **52**(6):781-788.
31. Hai-miao WU, Li-xin Z, Gui-ying YAO, Yan-wei Z, Guang-chao LIU: **Reliability Design Method Based on Average Safety Factor**. *Machine Design and Research* 2009, **25**(4):14-16.
32. Costigan PA, Deluzio KJ, Wyss UP: **Knee and hip kinetics during normal stair climbing**. *Gait & posture* 2002, **16**(1):31-37.
33. Dewidar M, Mohamed HF, Lim JK: **A New Approach for Manufacturing a High Porosity Ti-6Al-4V Scaffolds for Biomedical Applications**. *J Mater Sci Technol* 2008, **24**(6):931-935.
34. Van Bael S, Chai YC, Truscello S, Moesen M, Kerckhofs G, Van Oosterwyck H, Kruth IP, Schrooten J: **The effect of pore geometry on the in vitro biological behavior of human periosteum-derived cells seeded on selective laser-melted Ti6Al4V bone scaffolds**. *Acta biomaterialia* 2012, **8**(7):2824-2834.
35. Caparros C, Ortiz-Hernandez M, Molmeneu M, Punset M, Calero JA, Aparicio C, Fernandez-Fairen M, Perez R, Gil FJ: **Bioactive macroporous titanium implants highly interconnected**. *J Mater Sci-Mater M* 2016, **27**(10).
36. Wang C, Li X, Luo Y: **Design and Strength Analysis of Porous Titanium Scaffold**. *Journal of Shanghai Jiaotong University* 2016, **50**(2):165-168.
37. Arifvianto B, Leeflang MA, Zhou J: **Diametral compression behavior of biomedical titanium**

scaffolds with open, interconnected pores prepared with the space holder method. *Journal of the mechanical behavior of biomedical materials* 2017, **68**:144-154.

38. Zhang M, Wang GL, Zhang HF, Hu XD, Shi XY, Li S, Lin W: **Repair of segmental long bone defect in a rabbit radius nonunion model: comparison of cylindrical porous titanium and hydroxyapatite scaffolds**. *Artificial organs* 2014, **38**(6):493-502.

Figures

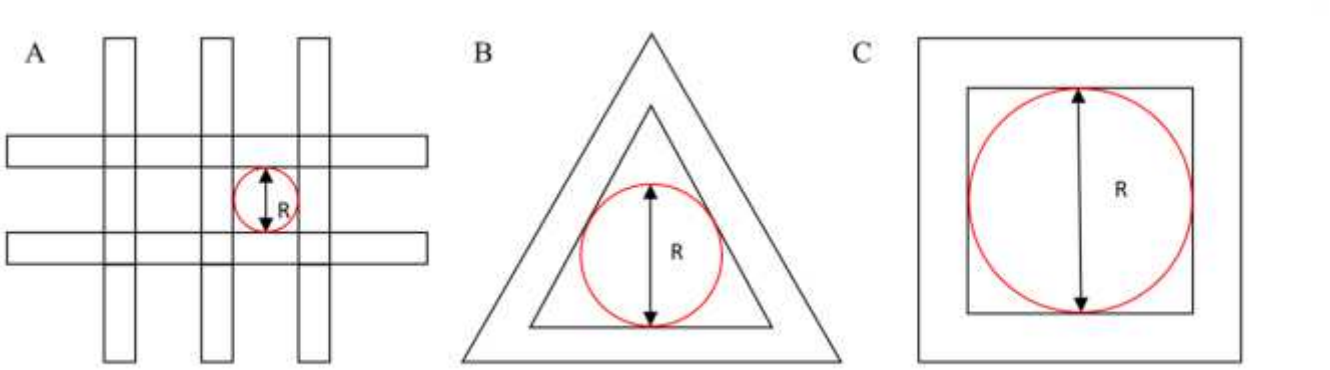

Figure 1

(a) Overall top view of the imitation diamond unit structure; R is the size of the aperture. (b) Regular tetrahedron unit structure has a diameter R in either side. (c) Size of the aperture R is the inscribed circle diameter on either side of the regular hexahedral unit structure.

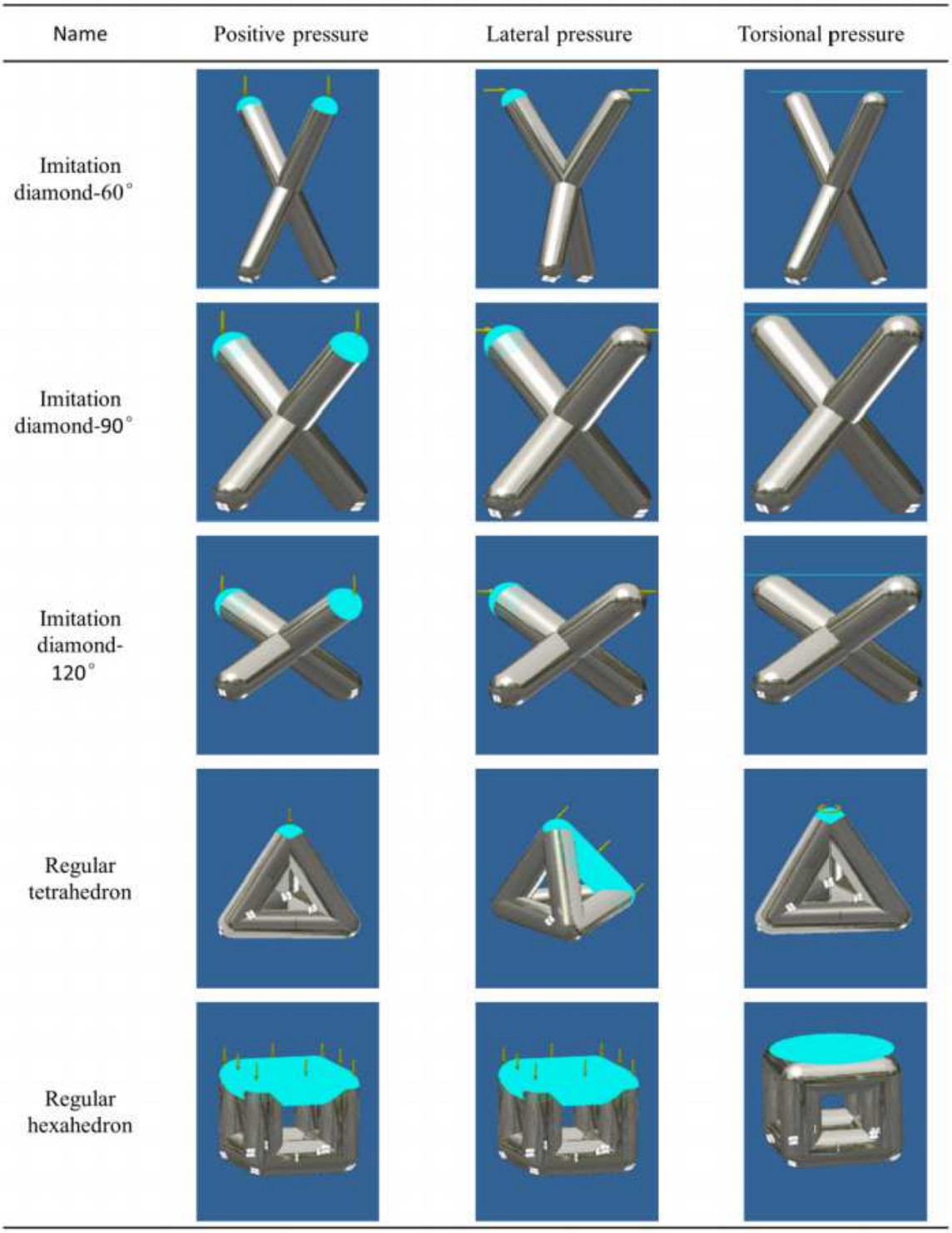

Figure 2

Schematic of different unit structures and applied pressure.

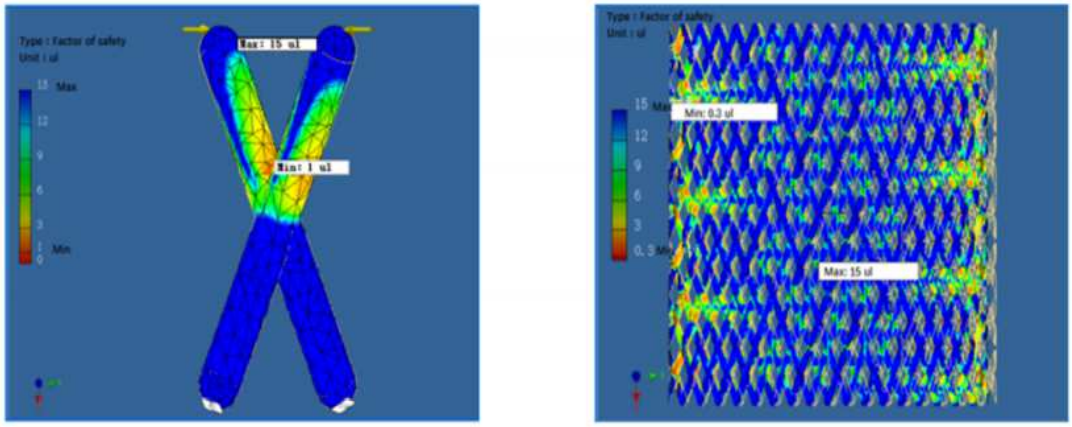

Figure 3

Unit structure and cylindrical structure of imitation diamond-60° under lateral pressure (600N); blue indicates security, and red indicates danger. The reddest point occurred when the safety factor was the smallest.

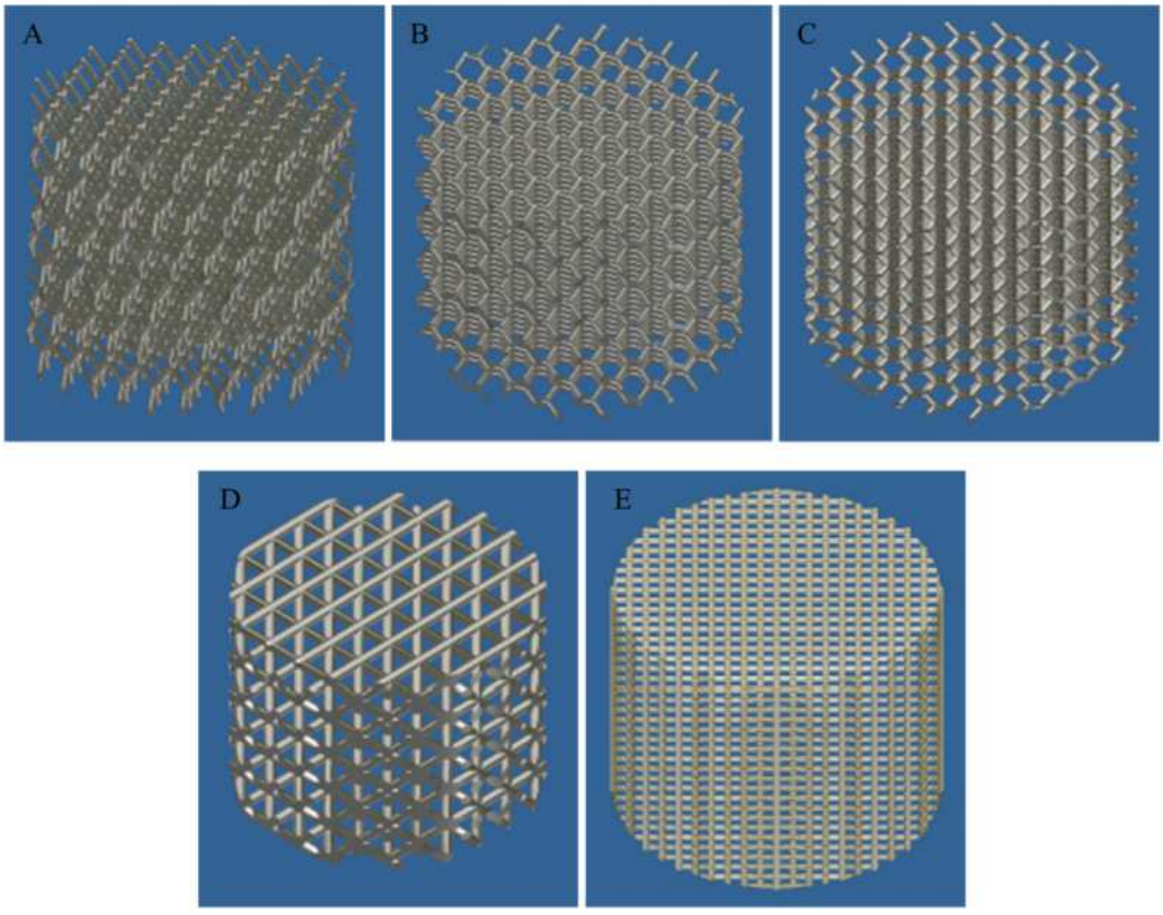

Figure 4

The five types of Cylindrical model. (A) Imitation diamond-60°; (B) imitation diamond-90°; (C) imitation diamond- 120; (D) regular tetrahedron: (E) hexahedron.

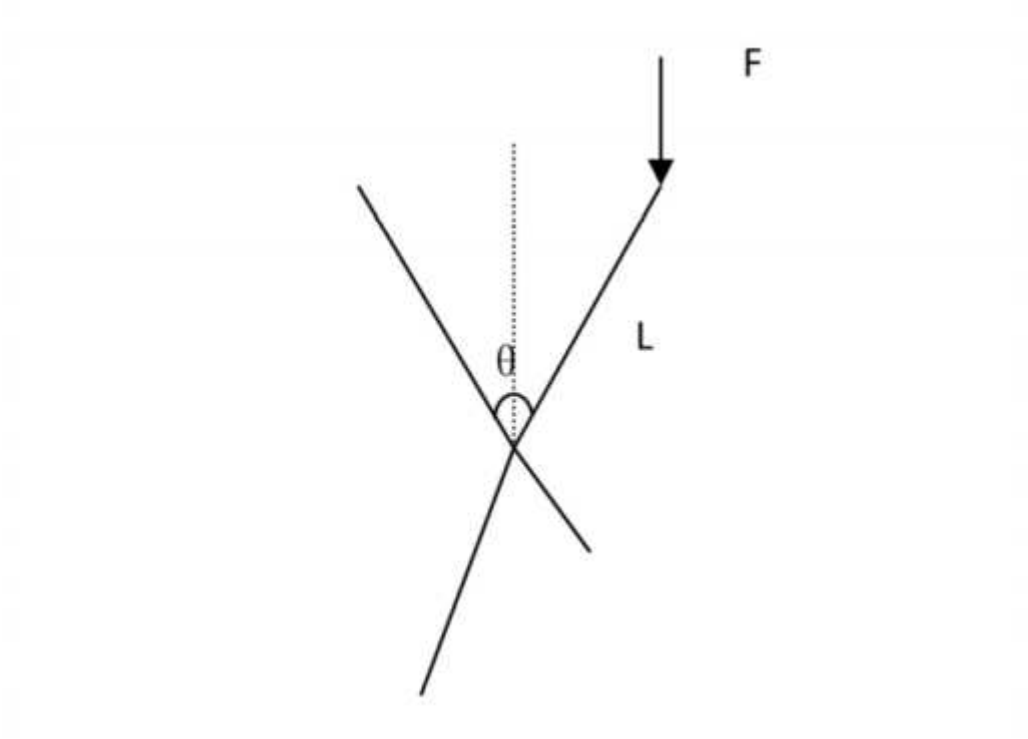

Figure 5

Positive pressure on the imitation diamond unit structure